

# Deformation of Jamaica and motion of the Gonâve microplate from GPS and seismic data

C. DeMets<sup>1</sup> and M. Wiggins-Grandison<sup>2</sup>

<sup>1</sup>Department of Geology and Geophysics, University of Wisconsin-Madison, Madison, WI 53706 USA. E-mail: chuck@geology.wisc.edu

<sup>2</sup>Earthquake Unit, University of the West Indies, Mona Campus, Kingston 7, Jamaica

Accepted 2006 September 11. Received 2006 September 6; in original form 2006 June 2

## SUMMARY

We use velocities from 20 GPS sites on the island of Jamaica and seismic data from the Jamaican Seismic Network to quantify motion of the proposed Gonâve microplate and study deformation and earthquake hazard in Jamaica. All 20 Jamaican GPS sites move significantly relative to both the Caribbean and North American plates, thereby confirming the existence of the Gonâve microplate. In a Caribbean Plate reference frame, the fastest site velocities in Jamaica are  $8 \pm 1 \text{ mm yr}^{-1}$ , representing a minimum estimate for the rate of Gonâve–Caribbean Plate motion. We estimate a firm upper limit of  $13 \pm 1 \text{ mm yr}^{-1}$  for Gonâve–Caribbean Plate motion assuming that additional elastic or permanent deformation occurs north of Jamaica beyond the reach of our GPS network. The range of estimates for Gonâve–Caribbean Plate motion exceeds the 3–7  $\text{mm yr}^{-1}$  range of geologically derived rates for post-10 Ma fault slip in Jamaica, suggesting that motion has either increased relative to the long-term deformation rate or that estimates of the long-term deformation rate are too slow. Minimum and maximum rates for Gonâve–North America Plate motion are  $6 \pm 1 \text{ mm yr}^{-1}$  and  $11 \pm 1 \text{ mm yr}^{-1}$  based on the differences between the estimated Gonâve–Caribbean rates and a recent GPS-based estimate of  $19.3 \pm 1 \text{ mm yr}^{-1}$  of Caribbean–North American Plate motion in Jamaica. These are slower than 15–20  $\text{mm yr}^{-1}$  published estimates of the long-term seafloor spreading rate across the Cayman spreading centre, which records Gonâve–North American Plate motion. Our observations are thus consistent with a model in which Gonâve–Caribbean Plate motion has increased through time while Gonâve–North America Plate motion has decreased, possibly reflecting a progressive transfer of slip from plate boundary structures that accommodate Gonâve–North America motion to faults that carry Gonâve–Caribbean Plate motion. In Jamaica, GPS site directions in both the Caribbean and North American Plate reference frames are parallel to the Caribbean–North America Plate slip direction and are only 10–20° different from the azimuths of the island’s major strike-slip faults. The mean *P*- and *T*-axes for 48 earthquakes since 1941 have near-horizontal plunges and are oriented 45° from the predicted plate slip direction. The kinematic and seismic data thus indicate that deformation on the island is dominated by left-lateral shear along largely E–W-trending strike-slip faults. Relative to the Caribbean Plate, the Jamaican GPS velocities exhibit a nearly monotonic increase in site velocities from south to north along a transect orthogonal to the island’s major E–W faults. This velocity gradient likely reflects the accumulation of elastic strain due to frictional locking of the major E–W faults. Velocities however also increase monotonically from the WSW to ENE along a transect orthogonal to the island’s numerous NNW-striking faults, consistent with the accumulation of significant elastic shortening along those faults and supportive of an interpretation of those faults as restraining bends. Seismic hazard assessment based on the GPS-derived deformation budget, likely maximum fault rupture lengths, and the historical seismic record suggests approximate repeat times of one to several centuries for earthquakes of maximum magnitudes of  $M_w = 7.0$ – $7.3$ . The strain that has accumulated since the destructive 1692 earthquake near the capital city of Kingston is presently sufficient to release a  $M_w = 7.2$  earthquake in eastern Jamaica.

**Key words:** Caribbean, Gonâve microplate, Jamaica, plate tectonics.

## 1 INTRODUCTION

An important objective of Global Positioning System (GPS) and seismic measurements in the northern Caribbean region is to better understand how motion across the Caribbean–North America Plate boundary is partitioned by the plate boundary structures and what this implies for local and regional tectonics and seismic hazard. Along the 1100-km-long stretch of the plate boundary that connects the Cayman spreading centre to faults in central Hispaniola, Caribbean–North America motion is partitioned between the Oriente fault, which follows the northern boundary of the Cayman Trough along much of its length (Fig. 1), and the Walton–Enriquillo–Plantain Garden fault zone, which collectively follow the southern boundary of the Cayman Trough. These faults also define the northern and southern boundaries of the elongate Gonave microplate, which is hypothesized by Mann *et al.* (1995) to have detached from the Caribbean Plate in response to the collision of the northern edge of the Caribbean Plate with the Bahama Platform in central Hispaniola. The hypothesized detachment of this microplate is estimated to have occurred as recently as the past  $\sim 5$  Myr (Mann *et al.* 1995) or as early as  $\sim 20$  Ma (Leroy *et al.* 2000). No well-constrained estimates of the Gonave microplate's present motion and rigidity are available due to a lack of GPS measurements from western Hispaniola and Jamaica, which are the only two substantial land masses that extend into the Gonave microplate.

The principal focus of this study, the island of Jamaica, extends  $\sim 230$  km along the Gonave–Caribbean Plate boundary (Figs 1 and 2) and straddles many and possibly all of the faults that accommodate Gonave–Caribbean Plate motion. Destructive historic earthquakes and abundant microseismicity (Wiggins-Grandison 2001) along faults exposed in and near Jamaica clearly indicate that faults on and near the island are active; however, the rate and distribution of fault slip are known only broadly from geological and structural studies of the island (e.g. Burke *et al.* 1980; Wadge & Dixon 1984; Mann *et al.* 1985) and mapping of nearby offshore faults (Leroy *et al.* 1996).

Here, we combine new velocities from a 20-station GPS network in Jamaica with seismologic data from the Jamaican Seismic Network (JSN) to study a variety of questions related to Gonave microplate motion and deformation of Jamaica. At a regional scale, we quantify how Caribbean–North American Plate motion is partitioned across the faults that border the Gonave microplate. This part of the analysis includes consideration of whether partitioning of slip between the northern and southern boundaries of the microplate has remained constant for the past few Myr or has changed, as might be expected if the Gonave microplate is gradually breaking away from the Caribbean Plate and accreting to the North American Plate (Mann *et al.* 1995).

At a local scale, we attempt to better quantify neotectonic deformation and seismic hazard in Jamaica. Twelve earthquakes with

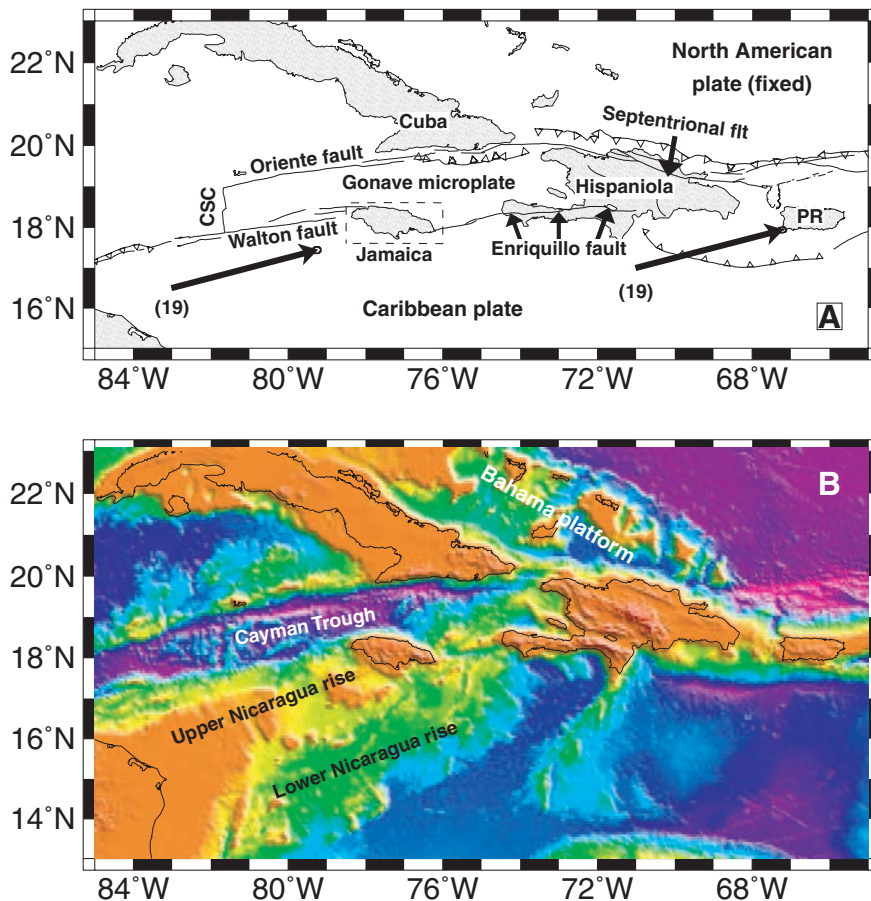


**Figure 1.** (a) Location map and tectonic setting for Gonave microplate and north central Caribbean. Arrows show Caribbean–North American Plate motion predicted by DeMets *et al.* (2006) model. Parenthetical numerals indicate rate in  $\text{mm yr}^{-1}$ . Uncertainty ellipses are 2-D, 95 per cent. Dashed rectangle indicates study area depicted in Fig. 3 and subsequent figures. CSC designates Cayman spreading centre and PR, Puerto Rico. (b) 2-min seafloor bathymetry and land topography from Sandwell & Smith (1997).

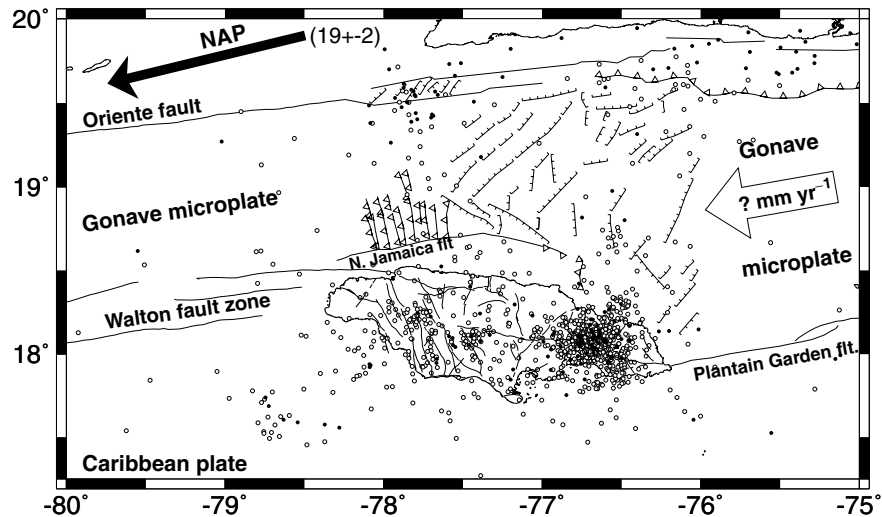


**Figure 2.** Faults and earthquakes in and near Jamaica and kinematic setting relative to stationary Caribbean Plate. Offshore faults are from Leroy *et al.* (1996) and onshore faults from Wiggins-Grandison & Atakan (2005). Open and filled circles, respectively, designate earthquakes located by the Jamaican Seismic Network from 1993 to 2004 and 1963 to 2005 teleseismically located earthquakes from the U.S. National Earthquake Information Centre epicentre file. Arrow specifying motion of North American Plate (NAP) is from model of DeMets *et al.* (2006). Rate is indicated in units of millimeters per year.

Modified Mercalli Intensities (MMI) between VII and X have struck Jamaica since 1667 (Wiggins-Grandison 2001), including the 1692 June 7 MMI X earthquake, which killed one-fourth of the population of Port Royal in southern Jamaica, and the 1907 January 14  $M = 6-6.5$  earthquake, which killed 1000 people and damaged or destroyed 85 per cent of the buildings in the capital city of Kingston. Our GPS measurements provide the first information about the rate that elastic strain is accumulating on the island, a key element of better understanding earthquake hazard in Jamaica.

## 2 SEISMOTECTONIC SETTINGS OF THE GONAVE MICROPLATE AND JAMAICA

### 2.1 Gonave microplate

The elongate Gonave microplate extends  $\sim 1100$  km west from the island of Hispaniola to the Cayman spreading centre (Fig. 1) and separates the Caribbean and North American plates everywhere along its length. Sinistral transcurrent faulting dominates motion along both its northern boundary with the North American Plate and its southern boundary with the Caribbean Plate (Fig. 1). Motion along its western and eastern boundaries consists of extension along the Cayman spreading centre and convergence in central Hispaniola, respectively. The northern boundary is defined primarily by the 950-km-long Oriente fault, which connects the northern end of the Cayman spreading centre to the Septentrional fault of northern Hispaniola. Earthquake focal mechanisms indicate that motion along this submarine boundary consists of pure left-lateral strike-slip motion west of south-central Cuba (Molnar & Sykes 1969; Van Dusen & Doser 2000; Moreno *et al.* 2002) and obliquely convergent motion along the Santiago Deformed Belt south of eastern Cuba (Calais & Mercier de Lepinay 1995; Van Dusen & Doser 2000; Moreno *et al.* 2002). Estimates of the long-term opening rate from the poorly expressed magnetic anomalies that flank the Cayman spreading centre range from 12 to 20 mm yr<sup>-1</sup> (Macdonald & Holcombe 1978; Rosencrantz & Sclater 1986; Leroy *et al.* 2000). High-resolution bathymetric mapping of the Cayman spreading cen-

tre reveals a seafloor morphology that is characteristic of an ultra-slow spreading centre (Ruellan *et al.* 2003), consistent with the slow opening rates indicated by the magnetic lineations.

Gonave microplate motion relative to the Caribbean Plate is accommodated by a series of faults that extend  $\sim 1100$  km eastward from the southern end of the Cayman spreading centre to southern Hispaniola. Between the Cayman spreading centre and western Jamaica, Gonave–Caribbean Plate motion occurs along the underwater Walton fault zone (Rosencrantz & Mann 1991). Slip along the Walton fault zone transfers in an unknown way to motion along a series of east-west-trending faults in Jamaica (Fig. 3) and possibly offshore faults that have been mapped with marine seismic profiles (Fig. 2) (Leroy *et al.* 1996). Slip along these faults is transferred eastward and southward across the Jamaican restraining bend (Horsfield 1974; Wadge & Dixon 1984; Mann *et al.* 1985; Leroy *et al.* 1996) to the Plantain Garden fault of eastern Jamaica (Figs 2 and 3) and continues eastward to a submarine connection with the Enriquillo fault of southern Hispaniola (Mann *et al.* 1995). Other faults more distant from the island accommodate an unknown amount of deformation, as indicated by the  $M = 6.5-7.0$  oblique thrusting earthquake in 1941 within the Nicaragua Rise  $\sim 100$  km southwest of Jamaica (Van Dusen & Doser 2000).

Estimates of the cumulative slip rate across the faults that accommodate Gonave–Caribbean Plate motion range from 4 to 20 mm yr<sup>-1</sup>. At the low end of these estimates, Burke *et al.* (1980) calculate an integrated slip rate of 4 mm yr<sup>-1</sup> for faults in Jamaica based on geologically mapped fault offsets and assumed offset ages. An independent, similarly slow 3–7 mm yr<sup>-1</sup> estimate of the slip rate along the Plantain Garden fault is based on the assumption that the 60-km-wide Morant pull-apart basin east of Jamaica and the 30–45 km offset of the eastern Jamaica shelf both occurred since  $\sim 9$  Ma (Natural Disaster Research *et al.* 1999). These geologically based estimates both agree within their uncertainties with a  $9 \pm 9$  mm yr<sup>-1</sup> GPS-based estimate of the slip rate along the eastern end of the Enriquillo fault in south-central Hispaniola (Calais *et al.* 2002). Sykes *et al.* (1982) estimate more rapid motion of 10–20 mm yr<sup>-1</sup> along the Enriquillo–Plantain Garden fault system from closure of the North America–South America–Caribbean Plate circuit.

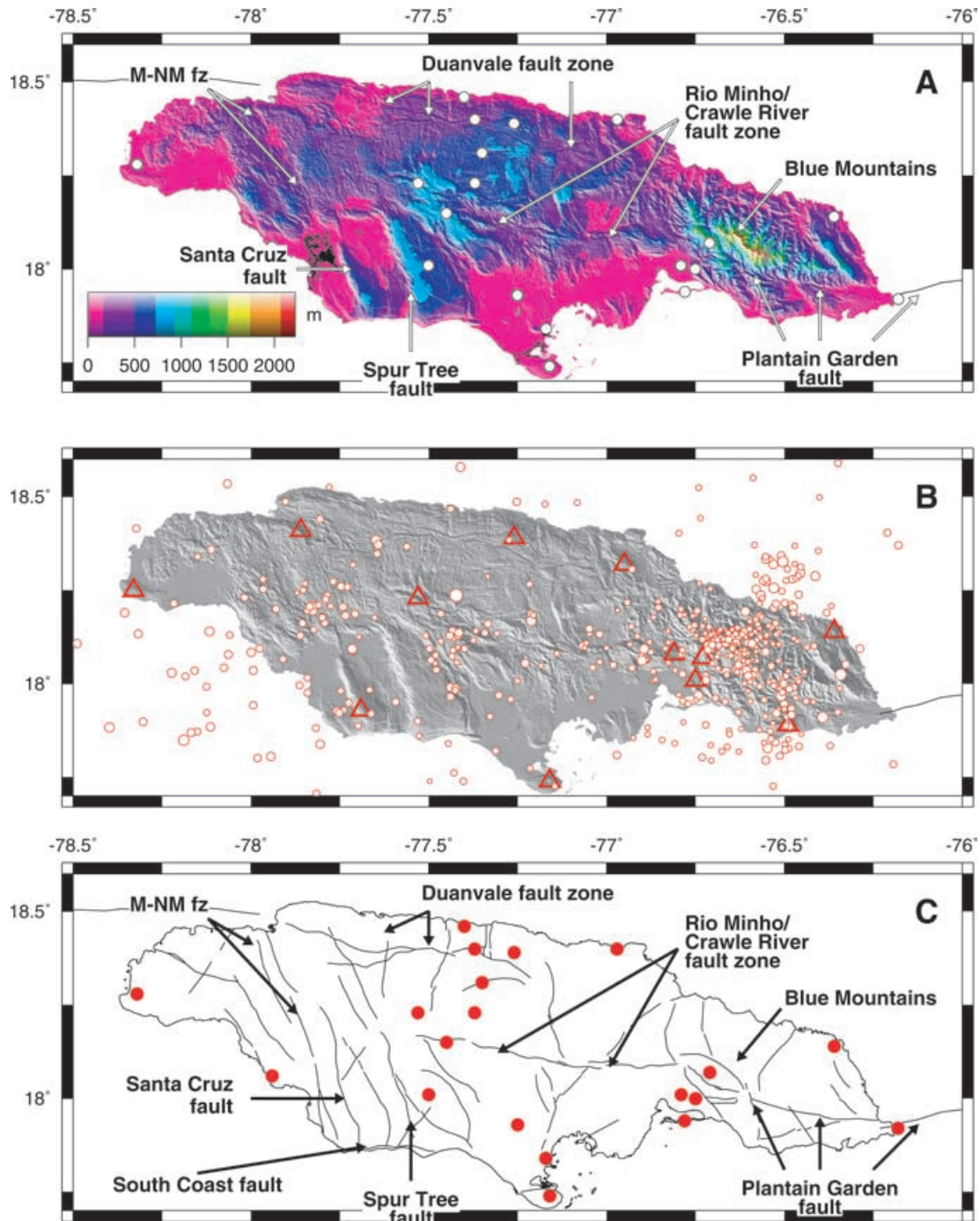


**Figure 3.** (a) Fault and GPS station locations overlaid on 90-m Space Shuttle Topographic Radar Mission (SRTM) topography illuminated from the southwest. M-NM fz is the Montpelier-New Marker fault zone. (b) The Jamaica Seismograph Network (triangles) and microearthquakes detected by four or more JSN stations for the period 1998–2004 (circles). Only earthquakes with magnitudes equal to or greater than 2.0 are shown, representing the average detection threshold for JSN. Epicentres also include the magnitude 5.1 earthquake of 2005 13 June in central Jamaica. Symbols are scaled to earthquake magnitudes. (c) Locations of GPS stations (red) and potentially active major faults.

## 2.2 Jamaica

The island of Jamaica is an emergent, uplifted part of the Nicaraguan Rise, a submarine volcanic plateau of intermediate thickness that extends southwest from the edge of the Cayman Trough (Fig. 1b). Tertiary limestones and inliers of the Cretaceous island-arc volcanic and volcanoclastic basement rocks that are exposed at the sur-

face (Robinson 1994) are offset by numerous faults, many with unknown present activity. The island's primary ~E–W-striking faults, the Plantain Garden, Duanvale, Rio Minho–Crawle River, and South Coastal faults (Fig. 3) (Horsfield 1974; Wadge & Dixon 1984; Mann *et al.* 1985), are connected by a series of NNW-striking faults that are presumed to transfer motion between them. Prominent amongst the NNW-trending faults are faults in the Blue Mountains of eastern

Jamaica, and the Spur Tree and Santa Cruz faults of central and western Jamaica (Fig. 3a). These faults are interpreted by Mann *et al.* (1985) as restraining bends that impede east-to-west sinistral shear across the island. The relative slip rates (and for some faults, the type of faulting) for the NNW-striking faults are unknown. Structural and palaeomagnetic data have also been used to support the existence of vertical axis block rotations in accommodating deformation (Ghose & Testamarta 1983; Draper & Robinson 1991).

An inversion of body wave traveltimes for locally recorded Jamaican earthquakes indicates that the crust consists of a 4–5-km-thick upper carbonate layer, an 18-km-thick intermediate layer with seismic velocities consistent with those of non-continental crust, and a 8-km-thick lower layer with velocities intermediate between those of oceanic crust and the upper mantle (Wiggins-Grandison 2004). The 30-km depth to the Moho derived from the tomographic inversion exceeds the 22-km depth to Moho derived from seismic imaging of offshore areas of the Nicaragua Rise (Arden 1975), but is consistent with evidence for several relocated earthquakes at depths of ~25 km (Wiggins-Grandison 2004).

### 3 GPS AND SEISMIC DATA

#### 3.1 GPS network description

The Jamaican GPS network consists of twenty geodetic benchmarks that span all of the major faults on the island (Table 1 and Figs 3a and c). Except for sites BAMB and JAMA, the benchmarks consist of 9-inch stainless steel pins or brass markers that are epoxied into carbonate bedrock or reinforced concrete structures. The pin at campaign site BAMB is in a large boulder located on a moderate slope. The antenna at site JAMA, which was installed by NOAA and is operated by the Jamaican Meteorological Service, is mounted on a 5-m-high steel tower bolted to the roof of a two-story building.

The GPS data consist of continuous observations at sites JAMA, PIKE, and PLND and episodic measurements at the remaining 17 benchmarks. All data were collected between early 1998 through early 2005 (Table 1 and Fig. 4). The 17 campaign sites were typ-

ically occupied continuously for 5–7 days in order to average the daily random noise down to 1–3 mm for a given site occupation. All campaign measurements were made with a Trimble 4000SSI dual-frequency code-phase receiver and choke ring antenna that was mounted on either a 0.50-m-high or 0.55-m-high spike mount. The equipment remained the same throughout the experiment, including the fixed height spike mount. As a consequence, the site coordinate time-series are not affected by errors due to incorrectly recorded antenna heights or mismodelled phase centres from different antenna types.

#### 3.2 GPS data analysis

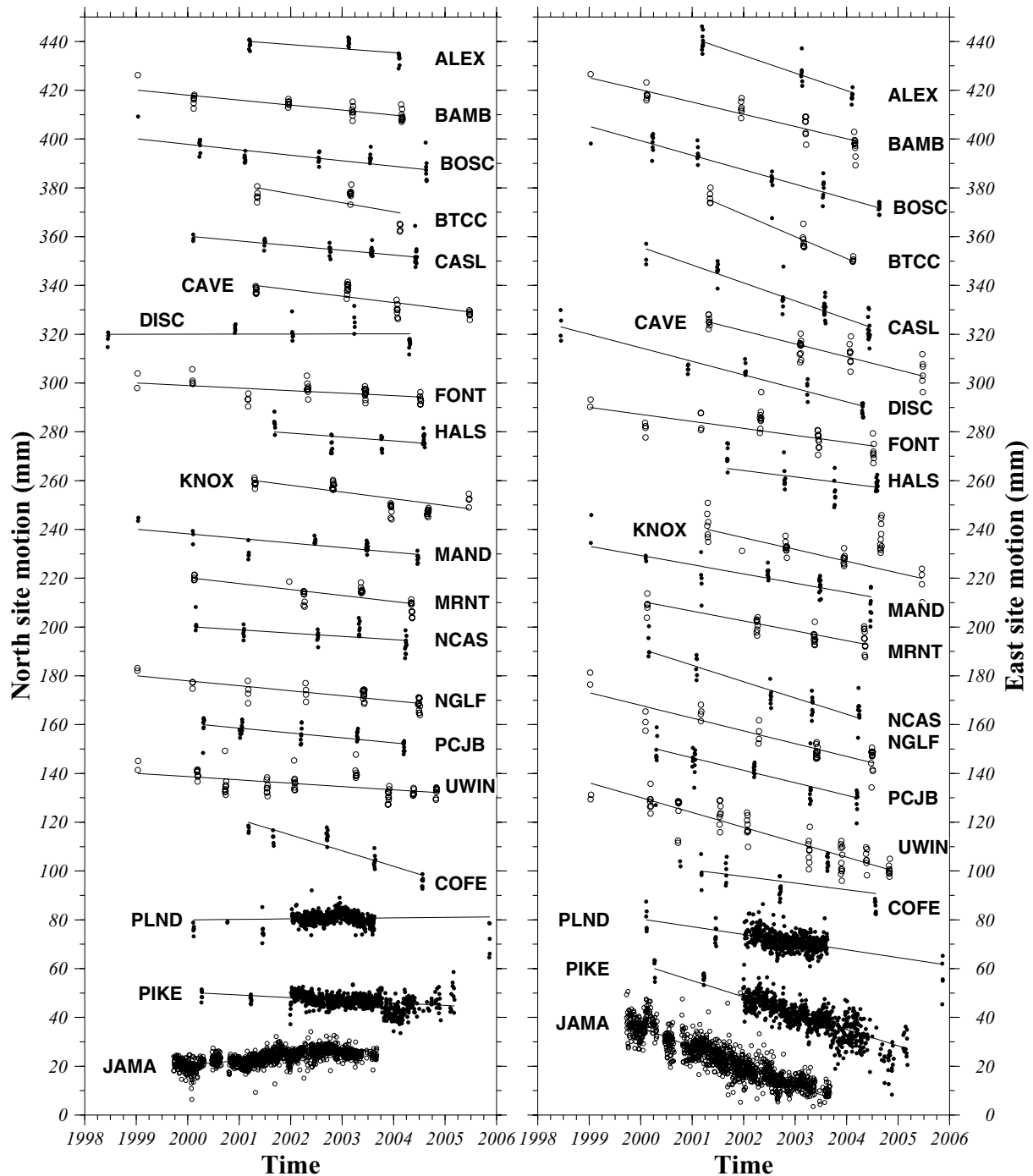
All GPS code-phase measurements were analysed using GIPSY analysis software from the Jet Propulsion Laboratory (JPL), free-network satellite orbits and satellite clock offsets obtained from JPL, and the precise point positioning analysis strategy described by Zumberge *et al.* (1997). Integer phase ambiguities were resolved when possible. Daily GPS station coordinates were first estimated in a non-fiducial reference frame (Heflin *et al.* 1992) and were then transformed to the International Terrestrial Reference Frame 2000 (ITRF2000) (Altamimi *et al.* 2002) using daily seven-parameter Helmert transformations supplied by JPL. We also estimated and removed daily and longer-period spatially correlated noise between sites using a technique described by Marquez-Azua & DeMets (2003). The day-to-day repeatabilities of the GPS site coordinates are 2–4 mm in latitude, 3–5 mm in longitude, and 8–10 mm in the vertical, typical for campaign observations.

Fig. 4 shows the north and east coordinate time-series relative to ITRF2000 for all 20 Jamaican GPS sites and best-fitting slopes estimated via linear regression of the site coordinate time-series (Table 1). Velocity uncertainties, which depend strongly on the time spanned by the observations at a given site, the number of site occupations, and the noise characteristics of a site's coordinate time-series, are estimated using an algorithm that accounts for all of these factors (Mao *et al.* 1999). Based on our own empirically estimated values for daily white noise, longer-period flicker noise, and an

Table 1. GPS station information.

Site name	Coordinates		Station days								Velocity <sup>a</sup>	
	Latitude (N)	Longitude (E)	1998	1999	2000	2001	2002	2003	2004	2005	North	East
alex	18.31	-77.35	-	-	-	9	-	7	7	-	6.4 ± 1.2	2.1 ± 1.5
bamb	18.39	-77.26	-	1	6	6	-	7	10	-	6.1 ± 0.5	4.3 ± 0.7
bosc	18.40	-76.97	-	1	8	8	7	8	8	-	6.0 ± 0.6	3.4 ± 0.7
btcc	18.40	-77.37	-	-	-	5	-	8	4	-	4.4 ± 1.8	0.2 ± 1.2
casl	18.14	-76.36	-	-	3	7	8	13	14	-	6.5 ± 0.6	2.1 ± 0.9
cave	18.23	-77.37	-	-	-	7	-	10	8	6	5.5 ± 0.9	4.0 ± 0.9
cofe	17.84	-77.17	-	-	-	10	11	8	7	-	1.7 ± 1.1	6.7 ± 1.6
disc	18.46	-77.40	4	-	5	-	6	5	10	-	8.1 ± 0.7	3.7 ± 0.6
font	18.06	-77.94	-	2	4	4	9	11	7	-	6.8 ± 0.6	6.5 ± 0.9
hals	17.93	-77.25	-	-	-	7	8	8	12	-	6.5 ± 1.3	6.9 ± 1.5
jama	17.94	-76.78	-	87	210	351	295	132	-	-	10.1 ± 0.7	1.6 ± 0.9
knox	18.15	-77.45	-	-	-	7	10	8	10	4	4.5 ± 1.0	7.5 ± 1.5
mand	18.01	-77.50	-	2	3	5	8	12	8	-	6.1 ± 0.8	5.7 ± 1.1
mrnt	17.92	-76.18	-	-	5	1	8	11	10	-	6.1 ± 0.7	5.5 ± 0.8
ncas	18.07	-76.71	-	-	5	6	7	8	11	-	7.0 ± 0.8	2.8 ± 1.1
nglf	18.28	-78.32	-	2	3	4	4	12	12	-	5.6 ± 0.7	4.1 ± 1.0
pcjb	18.01	-76.79	-	-	8	13	8	8	8	-	6.3 ± 0.7	4.4 ± 1.2
pike	18.23	-77.53	-	-	6	11	316	313	142	-	6.3 ± 0.7	1.8 ± 0.9
plnd	17.74	-77.16	-	-	8	9	305	216	-	-	8.7 ± 0.9	6.4 ± 0.7
uwin	18.00	-76.75	-	2	15	8	8	19	14	-	7.0 ± 0.8	3.4 ± 0.7

<sup>a</sup>Velocity units are in millimeters per year. Uncertainties are standard errors.



**Figure 4.** North and east components of GPS coordinate time-series for Jamaican sites. The slope of each site's time-series is reduced by the velocity predicted at the site for the Caribbean Plate relative to ITRF2000 (see text). Departures from zero slope thus represent movement of the site with respect to the Caribbean Plate interior.

assumed  $1 \text{ mm}/\sqrt{\text{yr}}$  of random monument wander, the estimated uncertainties in the north and east velocity components range from  $\pm 0.5\text{--}1.8 \text{ mm yr}^{-1}$ . Possible monument instability at some sites, particularly non-bedrock sites such as BAMB and JAMA, may cause systematic errors in those site velocities, but is difficult or impossible to quantify. We therefore exercise caution in our interpretation of any single station velocity.

Transformation of the site velocities from ITRF2000 into reference frames anchored to the Caribbean and North American Plate

interiors (Figs 5 and 6) is accomplished by appropriate vectorial addition of the observed site velocity and the motion that is predicted for a reference plate at each GPS site relative to ITRF2000. We describe motion of the Caribbean Plate relative to ITRF2000 using an angular velocity vector ( $36.3^\circ\text{N}$ ,  $98.5^\circ\text{W}$ ,  $0.255^\circ \text{ Myr}^{-1}$ ) that best fits the velocities of 15 Caribbean Plate GPS sites (DeMets *et al.* 2006). For the motion of the North American Plate relative to ITRF2000, we use an angular velocity vector ( $7.6^\circ\text{S}$ ,  $86.2^\circ\text{W}$ ,  $0.196^\circ \text{ Myr}^{-1}$ ) that best fits the velocities of 151 continuous GPS

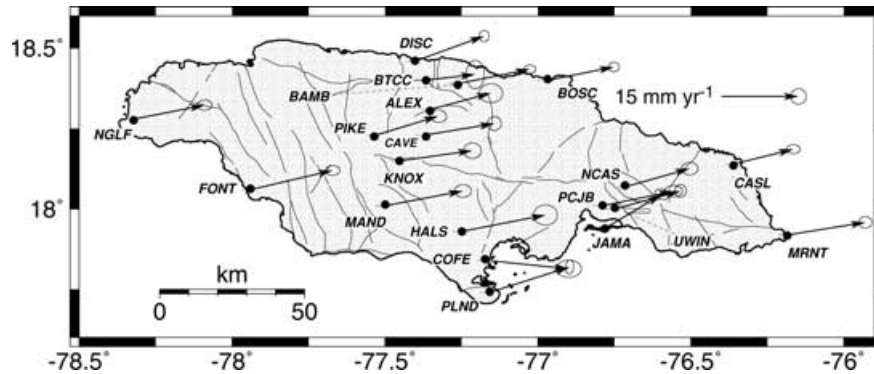


**Figure 5.** Jamaican GPS site velocities relative to North American Plate. North American Plate motion is specified by an angular velocity vector that best-fits the velocities of continuous sites from the North American Plate interior (see Section 3.2 in text). Error ellipses are 2-D,  $1\sigma$ . Four-letter site codes are from Table 1. Fault locations are from Fig. 3(c).

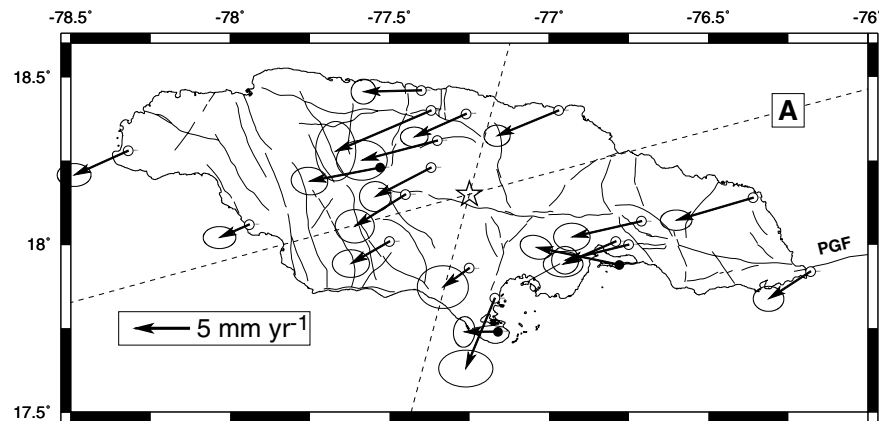


**Figure 6.** GPS site velocities relative to the Caribbean Plate, with 2-D standard error ellipses. Solid and open circles show locations of semi-continuous and campaign GPS sites, respectively. PGF marks offshore trace of the Plantain Garden fault. Star and dashed lines show origin and locations of velocity transects in Fig. 9.

stations from areas of the plate interior that are minimally affected by glacial isostatic rebound (DeMets *et al.* 2006). Uncertainties in the Caribbean and North American Plate angular velocity vectors are propagated into the GPS site velocity uncertainties to ensure that uncertainties in our plate-based reference frames are fully accounted for in the analysis. Uncertainties in the North American and Caribbean Plate angular velocity vectors increase the Jamaican site velocity uncertainties by less than 1 per cent and by 5–10 per cent, respectively, and hence do not constitute a limiting factor in our kinematic analysis.

### 3.3 Earthquake epicentres

The Jamaican Seismic Network (JSN) consists of twelve analogue short-period stations (Fig. 3b) with an average spacing of about 40 km. A typical station is equipped with a Mark Products vertical 1-Hz seismometer, Geotech amplifier-modulator and discriminator, and UHF radio and antenna. Four stations also have horizontal sensors. The signals are telemetered in real time to the central recording station in Kingston, where they are sampled at 50 Hz by an analogue-to-digital converter and a GPS time stamp is applied. Automatic digital recording with PC-SDA software (Malitsky & Shapira 1995) occurs once triggering thresholds are exceeded. Approximately 200 microearthquakes are presently recorded in or near Jamaica each year.

Since 1998, the first full year that JSN operated in its present configuration, more than 500 earthquakes of magnitude of 2.0 and higher have been located using four or more JSN stations (Fig. 3b). All earthquakes were located using a 1-D crustal velocity model from Wiggins-Grandison (2004). The earthquake coda magnitudes  $M_c$  are strongly correlated with moment magnitude  $M_w$  through the relation  $M_w = 0.92 \times M_c - 0.05$  (Wiggins-Grandison 2001).

Earthquakes since 1998 have occurred in most areas of the island and nearby offshore areas (Figs 2 and 3b), indicating that deformation is distributed between multiple faults. Most earthquakes in eastern Jamaica are associated with the topographically high Blue Mountains. In central and western Jamaica, most earthquakes are concentrated along and south of the centrally located Rio Minho-Crawle River fault zone, with lesser concentrations along the Spur Tree and Santa Cruz faults and the Montpelier-New Market fault belt in western Jamaica (Fig. 3b). The morphologically prominent Duanvale fault of northern Jamaica and Plantain Garden fault of eastern Jamaica are notably lacking in microseismicity, presumably because they are either creeping, inactive, or fully locked.

Significant numbers of offshore earthquakes also occur. An area of seismicity extends from Jamaica's northeastern coast (Fig. 2) to the southern coast of Cuba across the Gonave microplate interior (Moreno *et al.* 2002). These earthquakes correspond to a region of offshore faults that have been mapped with multichannel seismic profiles (Leroy *et al.* 1996), possibly defining a deforming area within the Gonave microplate. Significant seismicity south and

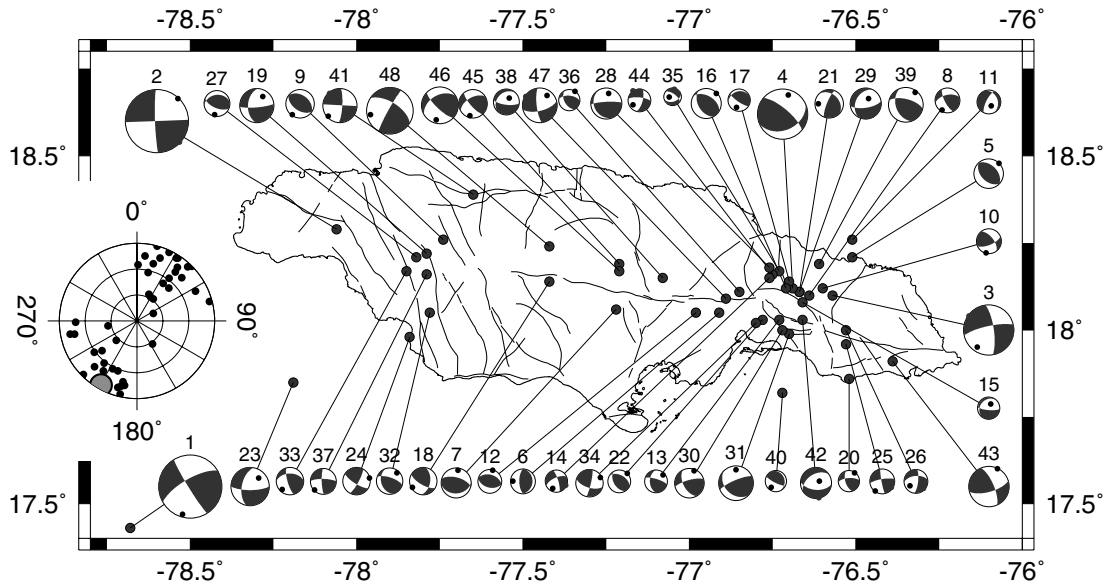


**Figure 7.** Earthquake focal mechanisms (Table 2) and major fault locations. Focal mechanisms #1–2 are from Van Dusen & Doser (2000), #3–4 from ISC data (Wiggins-Grandison 2001), and focal mechanisms #5–48 are derived from Jamaican Seismic Network data. Black dots in focal mechanisms indicate pressure axes. Focal mechanism size is scaled to earthquake magnitude. Polar plot on left side of map summarizes  $P$ -axis orientations for the individual earthquakes (small circles) and the mean  $P$ -axis orientation from the summed moment tensor inversion (large shaded circle).

southwest of the island, including a  $M = 6.5$ – $7.0$  earthquake in 1941  $\sim 100$  km southwest of the island (Van Dusen & Doser 2000), indicates that submarine faults are also active in these areas.

### 3.4 Earthquake focal mechanisms

Earthquake focal mechanisms provide valuable additional information about present deformation in Jamaica and are hence employed for our analysis. Figs 7 and 8 and Table 2 summarize all available earthquake focal mechanisms for Jamaica and vicinity. These include focal mechanisms for earthquakes recorded by the JSN between 1997 and 2005, many of which are re-interpreted from Wiggins-Grandison & Atakan (2005), focal mechanisms derived from ISC data for  $M = 5.5$  earthquakes that occurred in 1988 and 1993 (Wiggins-Grandison 2001), and focal mechanisms for the  $M = 6.5$ – $7$  earthquakes in 1941 and 1957 (Van Dusen & Doser 2000). The focal mechanisms we derived are restricted to earthquakes with good depth control and clear  $P$ -wave arrivals at a minimum of six seismographs (Fig. 8). All focal mechanisms were determined by searching through a plausible range of nodal plane orientations ( $10$ – $25^\circ$ ) for acceptable fits. Station polarities were calibrated periodically using distant events.

Most of the earthquakes have focal mechanisms that are consistent with left-lateral shear across E–W and WNW-striking faults. For example, the May 2003,  $M_L = 3.7$  earthquake along the Dunvale fault (solution 41), the May 2004,  $M_L = 4.4$  earthquake along the Plantain Garden fault (solution 43), and the June 2005,  $M_L = 5.1$  earthquake in central Jamaica (solution 48) each accommodated E–W to WNW–ESE sinistral slip.  $P$ -axis orientations for most earthquakes are accordingly oriented NNE to ENE (Fig. 7), consistent with regional accommodation of  $\sim$ E–W sinistral shear across the island. In Section 4.3, we analyse the revised and more numerous earthquake focal mechanisms given in Table 2 and confirm that faulting on the island is dominated by left-lateral,  $\sim$ E–W strike-slip motion, with a lesser component of NE–SW reverse faulting.

## 4 RESULTS

Our kinematic analysis is presented in three sections. In Section 4.1, we use the Jamaican GPS site velocities to test rigorously for the existence of the Gonave microplate, to examine the apparent significance of gradients in the GPS site velocities across the island, and to establish the minimum rate of Gonave microplate motion relative to the Caribbean Plate. In Section 4.2, site velocities relative to the North American Plate are used to determine minimum and maximum rates of motion across the Cayman spreading centre and Oriente fault, which define the western and northern boundaries of the microplate, respectively. In Section 4.3, we quantify seismic constraints on deformation of Jamaica and relate these to our geodetic measurements.

### 4.1 Jamaican GPS velocities relative to Caribbean Plate

#### 4.1.1 Kinematic test for existence of the Gonave microplate

Fig. 6 shows the velocities of the 20 Jamaican GPS sites relative to the Caribbean Plate interior. The site rates range from  $3 \pm 0.7$  mm yr $^{-1}$  in the southern and southwestern parts of the island to  $8$ – $10$  mm yr $^{-1}$  ( $\pm 1.4$  mm yr $^{-1}$ ) in northern and northeastern Jamaica. All twenty sites move significantly faster than their estimated standard errors. Eighteen of the twenty sites move southwest to west-southwest with respect to the Caribbean Plate, indicating that the predominant sense of deformation across the island is left-lateral.

We tested whether the motion of the Jamaican sites relative to the Caribbean Plate interior is statistically significant using an F-ratio test for the existence of an additional plate (Stein & Gordon 1984). Separate inversions of the 20 Jamaican site velocities (Table 1) and the velocities of 15 GPS sites in the Caribbean Plate interior (DeMets *et al.* 2006) for the angular velocity vector that best-fits each set of site velocities yields a summed least-squares misfit of  $\chi^2 = 131.4$ . In contrast, an inversion of the combined velocity subsets to estimate their best-fitting angular velocity vector,

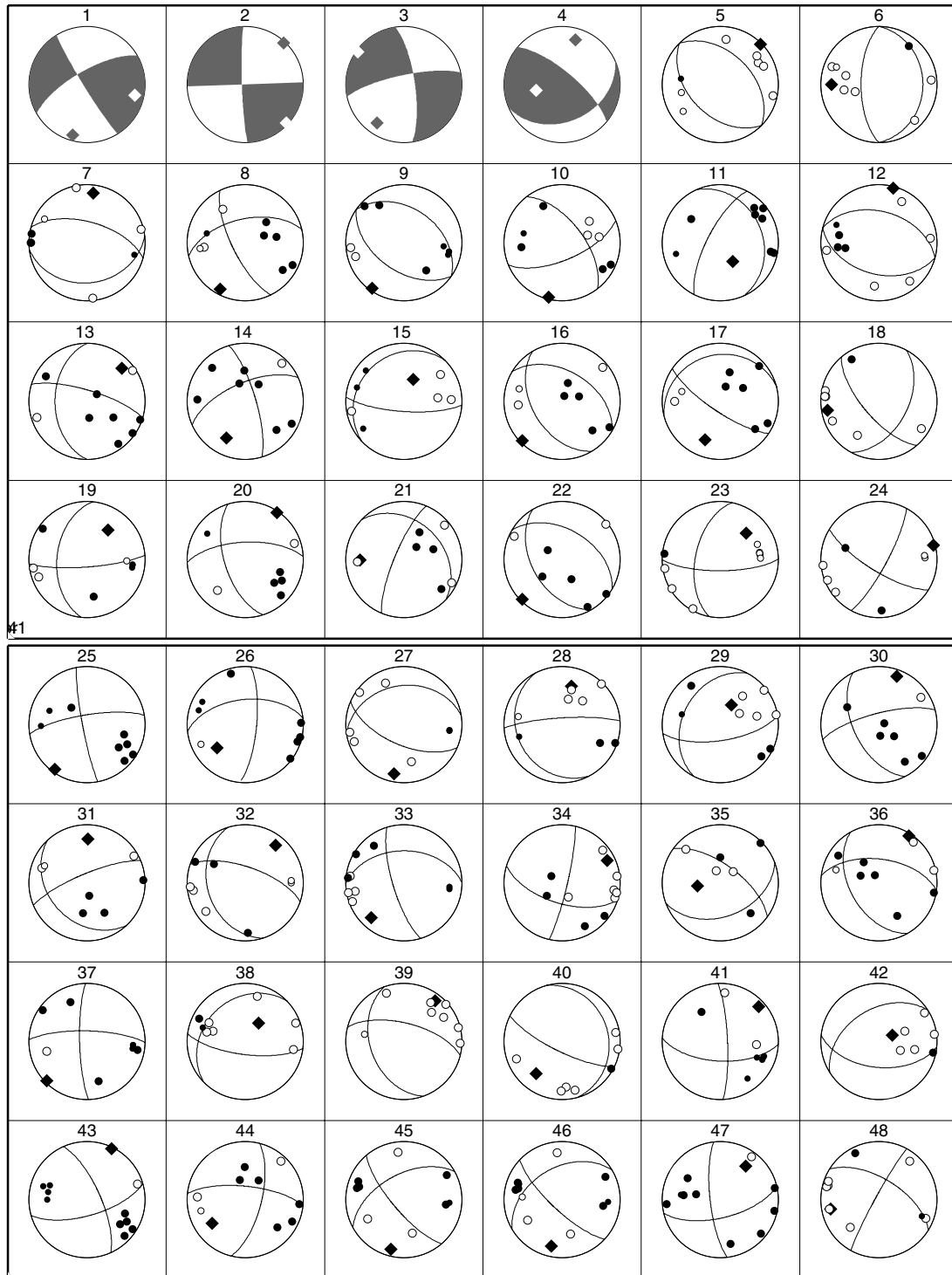


**Figure 8.** First motion arrivals and best-fitting nodal planes of focal mechanisms (Table 2) from Fig. 7. Focal mechanisms with grey-shaded quadrants are from other studies.

corresponding to a model in which the Gonâve microplate moves as part of the Caribbean Plate, gives  $\chi^2$  of 276.9. The probability that the factor-of-two improvement in the fit for the two- versus one-plate model is merely a random outcome of fitting the site velocities with one additional angular velocity vector is only two parts in  $10^{10}$ . The kinematic data thus strongly support the existence of an independently moving Gonâve microplate.

#### 4.1.2 Test for significant deformation within Jamaica

In a Caribbean Plate reference frame, the Jamaican site velocities increase systematically from rates of  $3 \pm 1$  mm yr<sup>-1</sup> at locations closest to the Caribbean Plate interior to rates of  $8 \pm 1$  mm yr<sup>-1</sup> at more distant locations (Fig. 6). Similar changes in the site velocities occur along a transect of the island that is parallel to the N75°E

**Table 2.** Earthquake source parameters.

Code	Date (year.month.day)	Hypocentre			$M_c$	Focal mechanism		
		Latitude (°N)	Longitude (°W)	Depth (km)		Strike	Dip	Rake
1	1941.04.07	17.43	-78.68	30	6.9	240	71	5
2	1957.03.02	18.29	-78.06	13	6.9	268	90	5
3	1988.11.12	18.10	-76.57	16	5.5	258	77	-16
4	1993.01.13	18.12	-76.69	12	5.5	66	36	31
5	1997.08.07	18.21	-76.51	19	3.2	135	45	90
6	1997.12.29	18.05	-76.91	17	2.7	0	25	90
7*	1998.01.15	18.06	-77.22	6	3.3	83	31	70
8*	1998.02.20	18.10	-76.64	19	2.7	257	56	23
9*	1998.02.23	18.26	-77.74	18	3.1	125	50	90
10*	1998.03.06	18.12	-76.60	18	2.7	67	66	33
11*	1998.03.24	18.26	-76.51	16	2.6	207	71	-69
12*	1998.03.29	18.05	-76.98	18	2.6	105	45	90
13*	1998.04.29	18.03	-76.73	13	2.5	287	75	48
14	1998.04.30	18.15	-76.76	18	2.4	245	64	-16
15*	1998.06.12	18.08	-76.66	10	2.4	94	76	-75
16*	1998.12.11	18.12	-76.71	25	3.3	300	47	69
17*	1998.12.13	18.14	-76.70	18	2.4	256	21	44
18*	1998.12.16	18.14	-77.42	22	3.0	140	68	46
19*	1999.01.24	18.22	-77.79	18	3.7	85	80	-44
20*	1999.02.28	17.86	-76.52	19	2.3	267	66	33
21*	1999.03.05	18.11	-76.67	16	3.1	313	33	24
22*	1999.07.11	18.03	-76.78	11	2.5	300	47	69
23	2000.02.07	17.85	-78.19	10	4.2	90	74	-37
24	2000.03.17	17.98	-77.84	16	3.0	122	74	12
25*	2000.03.31	17.96	-76.53	16	2.7	261	76	7
26	2000.04.09	18.00	-76.53	5	2.6	264	54	-20
27	2000.04.17	18.21	-77.82	17	2.8	261	33	62
28*	2000.04.18	18.18	-76.76	23	3.4	267	81	70
29	2000.06.15	18.11	-76.67	13	3.4	81	68	-63
30*	2000.09.06	18.00	-76.72	26	3.2	255	74	37
31*	2000.11.11	17.99	-76.70	13	3.8	247	77	59
32*	2001.05.03	18.05	-77.78	16	2.9	289	68	63
33*	2001.09.28	18.17	-77.85	15	3.0	270	44	22
34*	2001.10.24	18.02	-76.80	15	3.0	107	61	9
35*	2002.02.28	18.17	-76.73	22	1.9	306	64	-56
36*	2002.03.07	18.11	-76.85	24	2.3	277	56	53
37	2002.08.11	18.16	-77.79	18	2.8	271	76	11
38*	2003.01.07	18.15	-77.08	27	2.8	97	71	-69
39	2003.01.30	18.19	-76.61	13	3.8	284	64	56
40*	2003.02.27	17.82	-76.72	12	2.3	116	76	75
41	2003.05.15	18.39	-77.65	18	3.7	93	62	11
42	2003.12.15	18.03	-76.66	15	3.4	96	53	-65
43	2004.05.27	17.91	-76.39	18	4.4	74	68	20
44	2004.06.03	18.16	-76.75	18	2.5	276	71	-24
45	2004.08.10	18.19	-77.21	21	3.1	241	54	20
46	2004.08.10	18.17	-77.21	22	4.0	240	44	22
47	2004.08.14	18.09	-76.89	14	3.8	76	64	-16
48	2005.06.13	18.24	-77.42	17	5.1	302	61	6

Focal mechanism codes are tied to Figs 7 and 8. Earthquakes 1 and 2 are from Van Dusen & Doser (2000). Focal mechanisms for earthquakes that are marked by asterisks supersede those from Wiggins-Grandison & Atakan (2005).  $M_c$  are earthquake coda magnitudes (see text). Strike is measured clockwise from north. Dip is measured in degrees clockwise about the strike. Rake is measured as degrees counter-clockwise from strike in the specified nodal plane.

direction of predicted Gonâve–Caribbean Plate motion (Fig. 9a) and one that is perpendicular to the island’s principal ~E–W-striking faults (Fig. 9b), strongly suggesting that deformation on the island occurs along at least two sets of structures at high angles to each other. An inversion of the 20 Jamaican site velocities and their uncertainties to estimate an angular velocity vector that best-fits them in a weighted least-squares sense gives a weighted average misfit that is 1.8 times larger than the estimated velocity uncertainties. The GPS velocity field is thus misfit significantly if we assume that it

can be simplistically described by a rotation of a rigid block. We conclude that the apparent velocity gradients are highly significant with respect to the estimated velocity uncertainties.

#### 4.1.3 A lower bound for Gonâve–Caribbean Plate motion

The island-wide GPS velocity gradient and widespread seismicity in and near Jamaica indicate that deformation associated with Gonâve–Caribbean Plate motion is distributed across one or more faults that

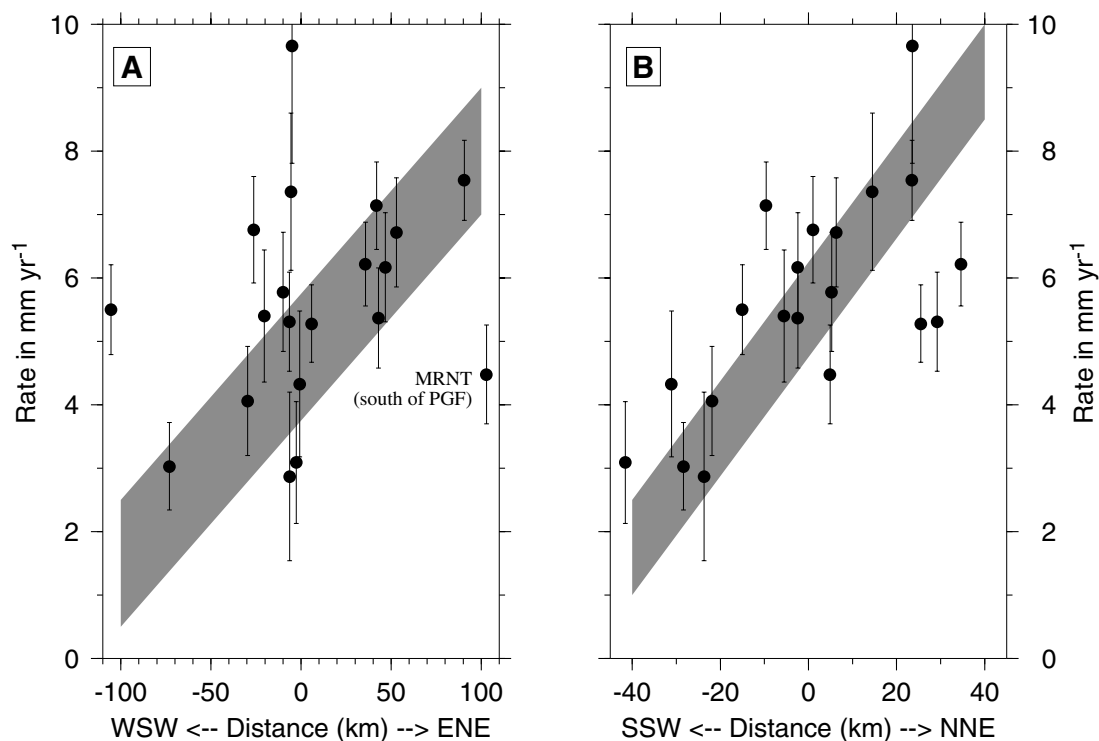


**Figure 9.** (a) Component of GPS velocities from Fig. 6 parallel to Caribbean–North America direction of  $N75^{\circ}E$ . Distance is measured along a  $N75^{\circ}E$  transect of Jamaica whose origin is shown by the star in Fig. 6. Uncertainties are 1-D, standard errors. (b) Same velocity components as shown in A, projected onto a  $N15^{\circ}E$  transect of Jamaica whose origin is shown by the star in Fig. 6. All site rates are given relative to a fixed Caribbean Plate.

are likely to be locked by friction at depth and are hence accumulating interseismic elastic strain. Since measurable elastic strain can extend outward from a locked fault to a distance of tens to hundreds of kilometers from the fault (see below), it is unlikely that any of our Jamaican GPS sites lie outside this deforming zone and hence fully sample the motion of the Gonâve microplate interior. We can nonetheless estimate a minimum rate for Gonâve–Caribbean Plate motion from the velocities of sites in northern and eastern Jamaica, which lie the closest to the interior of the Gonâve microplate. These range from  $5.5 \pm 0.8$  to  $9.8 \pm 1.4$   $\text{mm yr}^{-1}$  (Figs 6 and 9b) for sites in northern Jamaica, to  $7 \pm 1$  to  $7.5 \pm 1$   $\text{mm yr}^{-1}$  (Figs 6 and 9a) for sites in eastern Jamaica. Within their uncertainties, both groups of sites move at a rate of  $8 \pm 1$   $\text{mm yr}^{-1}$  relative to the Caribbean Plate interior, constituting a useful minimum estimate for the rate of the Gonâve Plate interior relative to the Caribbean Plate.

Although by definition our GPS measurements are limited to onshore areas, any deformation that occurs south of the island is implicitly captured by the Jamaican site velocities because the GPS site velocities can be referenced to the well-known motion of the Caribbean Plate interior (Figs 6 and 9). In contrast, any deformation that occurs north of the island across faults such as the North Jamaica fault (Fig. 2) (Leroy *et al.* 1996) or due to interseismic elastic strain that is accumulating in offshore areas due to locked fault(s) on land cannot be measured because no independent estimate of Gonâve Plate motion relative to ITRF2000 is available. As a consequence, a fundamental unknown in the analysis that follows is how much if any long-term or interseismic elastic deformation is accommodated north of Jamaica in the Cayman Trough.

Elastic half-space modelling can be used to approximate how much interseismic elastic deformation might be occurring north of Jamaica. If we simplistically assume that most plate boundary

deformation in Jamaica is focused along a strike-slip fault that is located near the central axis of the island (e.g. the Rio Minho–Crawle River fault zone shown in Fig. 3), and further assume that such a fault is locked to depths of 20 km, in crude agreement with the  $\sim 8$ –25 km depths of relocated microseisms (Wiggins–Grandison 2004), then approximately 75 per cent of the interseismic elastic deformation is predicted to accumulate within a 80 km-wide zone that is centred on the fault. Given Jamaica's comparable north-south dimension of 85 km and a long-term slip rate of  $8 \text{ mm yr}^{-1}$  along this fault, our results imply that  $\sim 25$  per cent or  $\sim 2 \text{ mm yr}^{-1}$  of this elastic strain would occur offshore, half to the north of the island. The minimum implied rate of long-term Gonâve–Caribbean motion would thus be  $9 \text{ mm yr}^{-1}$ , representing the  $8 \text{ mm yr}^{-1}$  of observed slip and an additional  $1 \text{ mm yr}^{-1}$  of unrecorded elastic deformation north of the island.

Given the numerous unknowns about the locations and slip rates of the active faults and their locking depths, the above exercise emphasizes the difficulty in estimating a ‘best’ rate for Gonâve–Caribbean Plate motion via modelling of the Jamaican GPS velocity field. Given these unknowns and the still-large uncertainties in the velocities for many of our GPS sites, we defer such modelling to a future paper and proceed with our kinematic analysis based on the  $8 \pm 1 \text{ mm yr}^{-1}$  minimum rate that we estimate for Gonâve–Caribbean Plate motion from the velocities for sites in northern and eastern Jamaica.

#### 4.2 Gonâve microplate motion relative to the North American Plate

The average direction of motion for the 20 Jamaican GPS sites relative to the North American Plate is  $N77.1^{\circ}E \pm 0.8^{\circ}$  (Fig. 10a), the

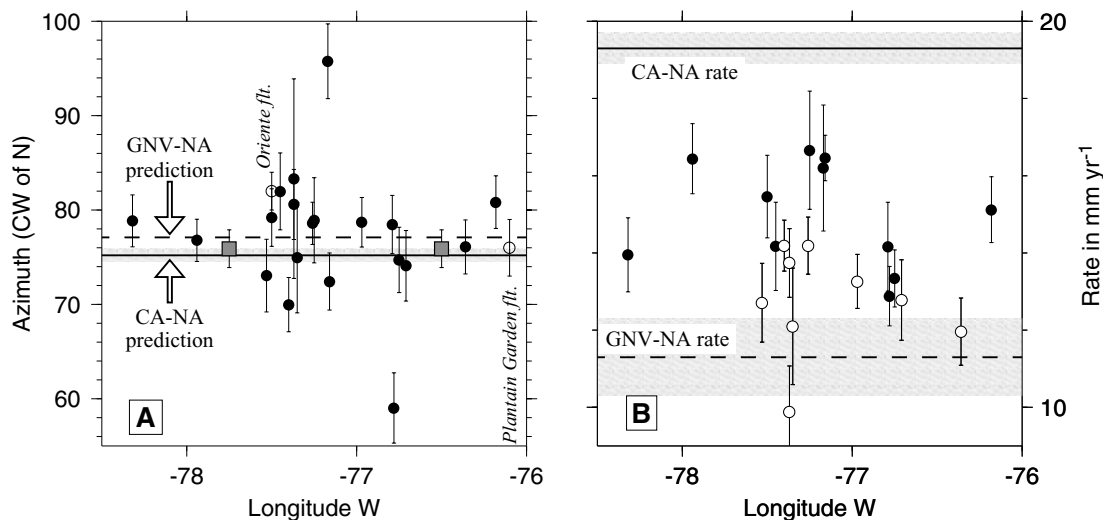


**Figure 10.** (a) GPS site directions (solid circles) relative to North American Plate and measured azimuths for the Oriente and Plantain Garden faults (open circles). Squares show direction of strike-slip motion inferred from the summed seismic moment tensor for 1988–2005 Jamaican earthquakes (see text). Motion and standard errors for the Caribbean–North America (CA-NA) and Gonâve–North America (GNV-NA) directions are shown by the solid and dashed lines and shaded region. (b) GPS site rates relative to North American Plate. Solid and dashed lines and shaded regions show motions and uncertainties for rates of Caribbean–North America and Gonâve–North America motions predicted in central Jamaica. Open and filled circles show sites located northeast and southwest of the dashed line shown in Fig. 6. Gonâve–North America rate represents maximum estimate based on  $8 \pm 1 \text{ mm yr}^{-1}$  minimum estimate for the Gonâve–Caribbean rate discussed in the text.

same within uncertainties as the  $N75.2^\circ E \pm 0.7^\circ$  direction predicted by the best-fitting Caribbean–North America angular velocity vector of DeMets *et al.* (2006). The Jamaican GPS sites thus move parallel to the direction predicted by a Caribbean–North America Plate angular velocity vector even though those sites lie along the Caribbean–Gonâve Plate boundary. This requires that motion of the Gonave Plate relative to the Caribbean Plate is parallel to Gonave–North America motion. That the Oriente and Plantain Garden faults, which respectively, accommodate Gonâve–North America and Gonâve–Caribbean Plate motion, are both also parallel within errors to the Jamaican GPS site directions and Caribbean–North American Plate motion (Fig. 10a) further corroborates evidence that deformation associated with motion of the Caribbean–North America–Gonâve Plate system is dominated by shear.

The  $N77.1^\circ E \pm 0.8^\circ$  average direction for the 20 Jamaican GPS sites relative to the North American Plate and azimuths of the Oriente strike-slip fault given in the NUVEL-1 data set (DeMets *et al.* 1990) constrain the direction of Gonâve microplate motion relative to the North American Plate at several different locations and hence can be used to estimate the angular velocity vector that describes motion of the Gonâve Plate relative to North America. An inversion of these observations and their uncertainties yields a best-fitting pole located at  $20^\circ S, 71^\circ W$ . Along the Gonâve–North America Plate boundary, this pole defines a small circle that is concave to the south, mirroring the curvature of the Oriente fault.

Minimum and maximum rates of angular rotation about this pole are  $-0.085 \pm 0.015^\circ \text{ Myr}^{-1}$  and  $-0.16 \pm 0.02^\circ \text{ Myr}^{-1}$  and are determined as follows. The maximum rate is inferred from the vector difference between the  $8 \pm 1 \text{ mm yr}^{-1}$  minimum slip rate we estimate for Gonâve–Caribbean motion in Jamaica (Section 4.1) and the  $19.3 \pm 0.4 \text{ mm yr}^{-1}$  Caribbean–North American Plate rate predicted in central Jamaica by the GPS-based model of DeMets *et al.* (2006). The  $11 \pm 1.1 \text{ mm yr}^{-1}$  difference between these two rates represents a maximum estimate for Gonâve microplate motion relative to the

North American Plate in Jamaica. For a best-fitting Gonâve–North America pole that is located at  $20^\circ S, 71^\circ W$ , an angular rotation rate of  $-0.16 \pm 0.02^\circ \text{ Myr}^{-1}$  is required to predict motion of  $11 \pm 1.1 \text{ mm yr}^{-1}$  in Jamaica.

Determining the minimum rate for Gonâve–North America Plate motion requires estimating an upper bound for Gonâve–Caribbean Plate motion. Although an unique upper bound cannot be estimated because of the unknown amount of deformation that occurs north of Jamaica (Section 4.1.3), an upper bound can nonetheless be approximated by assuming a model that maximizes the amount of hypothetical interseismic elastic deformation that might be occurring north of Jamaica due to interseismic locking of onshore faults. Assuming that all Gonâve–Caribbean motion at the longitude of central Jamaica is presently focused along the Duanvale fault of northern Jamaica, the  $6\text{--}7 \text{ mm yr}^{-1}$  of elastic deformation recorded by GPS sites located south of the Duanvale fault (Figs 9 and 10b) should be mirrored by  $6\text{--}7 \text{ mm yr}^{-1}$  of additional elastic deformation north of the fault assuming that deformation is symmetric with respect to the Duanvale fault. This model implies there is a total of  $12\text{--}14 \text{ mm yr}^{-1}$  of integrated elastic deformation across the Gonâve–Caribbean Plate boundary zone, equal to  $13 \pm 1 \text{ mm yr}^{-1}$  within the errors of our measurements and assumptions. Relative to the  $19.3 \pm 0.4 \text{ mm yr}^{-1}$  Caribbean–North American Plate rate that is predicted for central Jamaica, the  $13 \pm 1 \text{ mm yr}^{-1}$  approximate upper bound for Gonâve–Caribbean motion implies a  $6 \pm 1 \text{ mm yr}^{-1}$  minimum rate for Gonâve–North American Plate motion in Jamaica. For a best-fitting Gonâve–North America pole that is located at  $20^\circ S, 71^\circ W$ , the implied minimum angular rotation rate is  $-0.085 \pm 0.015^\circ \text{ Myr}^{-1}$ .

In summary, the Jamaican GPS site motions imply a relatively firm maximum rate of  $11 \pm 1 \text{ mm yr}^{-1}$  for Gonâve–North American Plate motion and a more uncertain, assumption-dependent minimum rate of  $6 \pm 1 \text{ mm yr}^{-1}$ . We discuss the tectonic implications of the minimum and maximum rates in Section 5.2.

### 4.3 Comparison of seismic and geodetic observations

We next use seismic data for an independent view of the present deformation regime in Jamaica. To do so, we assume that the earthquake focal mechanisms presented in Table 2 and Fig. 7 are characteristic of the long-term seismicity and hence state of stress on the island. For each of the 48 earthquake focal mechanisms, we calculated its corresponding seismic moment tensor. We then summed the 48 seismic moment tensors and derived the orientations and relative magnitudes of the principal ( $P$ ,  $T$ , and  $B$ ) stress axes for the summed moment tensor. The resulting stress axes represent the mean principal stress directions and implicitly weight the information from individual earthquakes by their estimated moments. The stress axes are dominated by stress that was released by the earthquakes in 1941 and 1957, whose seismic moments are  $\sim 3$  orders of magnitude larger than those for the smallest earthquakes included in our analysis.

The  $P$ -axis derived from the summed moment tensor has an azimuth of  $N29.5^\circ E$  and a nearly horizontal plunge of  $5^\circ$  (Fig. 7). The  $T$ -axis has an azimuth of  $N61.4^\circ W$  and also has a nearly horizontal plunge ( $9^\circ$ ). If we exclude the moment tensors for the 1941 and 1957 earthquakes, which otherwise comprise more than 99 per cent of the summed seismic moment, the  $P$ - and  $T$ -axis orientations for the remaining 46 earthquakes change by only  $2^\circ$  CW in the azimuth and  $4^\circ$  in the plunge. The principal stress axes are thus nearly horizontal, indicative of a deformation regime dominated by strike-slip faulting. This agrees with results reported by Wiggins-Grandison & Atakan (2005), who estimate best principal stress axes from the focal mechanisms of 19 earthquakes from eastern Jamaica, six earthquakes from central Jamaica, and four earthquakes from western Jamaica, and conclude that seismically recorded deformation is consistent with a strike-slip fault regime over much of the island, including nearly horizontal maximum principal stresses.

We also derived separate summed moment tensors for earthquakes from eastern Jamaica and earthquakes from the remainder of the island to test whether the mean  $P$  and  $T$  axes change significantly with location. The mean  $P$  and  $T$  axes for those two regions differ by only  $3^\circ$  in azimuth and insignificantly in plunge. Evidence for deformation that is dominated by strike-slip faulting is thus robust and island-wide. This differs from results reported by Wiggins-Grandison & Atakan (2005), who find apparent differences in the mean stress axes from different parts of Jamaica and conclude that the island's stress regime varies by location. We suspect that the absence of evidence for significant regional differences in the mean principal stresses in our data results from the larger number of focal mechanisms that we employ and revisions that we have made to many of the focal mechanisms that were employed by Wiggins-Grandison and Atakan.

If we simplistically assume that the nearly horizontal principal stresses are resolved on average onto vertical strike-slip faults that trend  $45^\circ$  from the  $P$ -axis orientation, the implied sense of slip and slip direction for deformation is left-lateral and  $N74.5^\circ E \pm 2^\circ$  (Fig. 10). The direction of motion is parallel within uncertainties to the  $N75.2^\circ E \pm 0.7^\circ$  Caribbean–North America direction, and the motions of the Jamaican GPS sites relative to both the Caribbean and North American plates (Fig. 10a). The close agreement between the directions of motion indicated by these three independent types of measurements (e.g. seismic, GPS in Jamaica, and plate-scale GPS) suggests that most present-day deformation in Jamaica is driven by sinistral shear between the Caribbean and North American plates.

The  $N74.5^\circ E$  direction inferred from the stress axes of the summed seismic moment tensor agrees within uncertainties with the  $N70^\circ E \pm 4^\circ$  average direction exhibited by the Jamaican GPS sites relative to the Caribbean Plate, but forms an angle of  $\sim 15^\circ$ – $25^\circ$  with respect to the azimuths of the island's primary strike-slip faults, which trend from E–W to WSW–ENE (Fig. 3). If we assume an average azimuth of  $S80^\circ E$  for the principal strike-slip faults, the  $8 \text{ mm yr}^{-1}$  minimum slip rate for Gonâve–Caribbean motion resolves into a  $7 \text{ mm yr}^{-1}$  fault-parallel component and  $3 \text{ mm yr}^{-1}$  fault-normal component (both minimum rates). Whether the fault-normal and fault-parallel components are accommodated by the same faults or are instead partitioned between differing sets of structures is unknown.

## 5 DISCUSSION

### 5.1 Earthquake hazard assessments

Our  $8 \pm 1 \text{ mm yr}^{-1}$  estimate for the minimum rate of Gonâve–Caribbean Plate motion in Jamaica provides a useful starting point for earthquake hazard assessment in Jamaica, particularly given the lack of palaeoseismologic constraints on fault rupture histories and the dearth of geological and geodetic information about individual fault slip rates in Jamaica. Below, we quantify the amount of unrelieved fault slip and hence unrelieved seismic moment since the 1692 Port Royal and 1907 Kingston earthquakes, which were the two most damaging historic earthquakes on the island. The moment magnitudes for historic earthquakes are from an earthquake catalogue for Jamaica that is maintained for seismic hazard analysis by one of us (M. Wiggins-Grandison).

#### 5.1.1 Eastern Jamaica

Although the fault that ruptured in the 1692 earthquake that destroyed Port Royal is unknown, the earthquake triggered the Judgement Cliff landslide along the western trace of the Plantain Garden fault (Tomblin & Robson 1977). Historical reports indicate that this landslide killed 19 people, displaced the land surface in some areas by 0.8 km, and induced sufficient subsidence near Port Morant in eastern Jamaica, where the Plantain Garden fault comes onshore, to create a large lake in an area that was formerly above ground (Tomblin & Robson 1977). This suggests that the 1692 earthquake ruptured the Plantain Garden fault. Because this fault runs close to the capital city of Kingston, estimating a maximum plausible rupture magnitude for future earthquakes on this fault is important. If we assume that its maximum likely rupture length extends approximately 70 km from the Morant pull-apart basin in the Jamaica Passage east of the island to the fault restraining bend near Kingston, and further assume that the seismogenic zone extends over a depth range of 15 km, comparable to that for the May 28, 2004 strike-slip earthquake on the Plantain Garden fault (event #43 in Fig. 7), then the implied fault-surface area available for seismogenic rupture of the Plantain Garden fault is about  $1000 \text{ km}^2$ . For a minimum slip rate of  $8 \text{ mm yr}^{-1}$  and assumed shear modulus of 30 GPa, the annual rate of increase in the seismic moment deficit is  $2.4 \times 10^{17} \text{ N m}$ . The seismic moment deficit that has accumulated since 1692 is thus  $7.5 \times 10^{19} \text{ N m}$ , equivalent to 2.5 m of unrelieved surface slip. Assuming a standard moment-magnitude relation of  $M_w = \log(M_o)/1.5 - 10.73$  (Hanks & Kanamori 1979), the unrelieved elastic strain could release the equivalent of a  $M_w = 7.2$ – $7.3$  earthquake.

Enough elastic strain has thus accumulated since 1692 along the Plantain Garden fault to yield a major earthquake. Assuming that the maximum theoretical magnitude for the ~70-km-long Plantain Garden fault is  $M_w = 7.0\text{--}7.3$ , which is typical for faults with maximum surface rupture lengths of 30 km to 70 km (Wells & Coppersmith 1994) and that strain accumulates at the rate specified in the previous paragraph, the implied range of recurrence intervals for earthquakes in this magnitude range is 165 yr to 460 yr. If the characteristic earthquake along the Plantain Garden fault is instead only  $M_w = 6.5$ , equal to the approximate magnitude of the 1907 Kingston earthquake (Wiggins-Grandison 2001), then the implied recurrence interval is only 30 yr. The historic earthquake record does not support such a short recurrence interval.

Numerous unknowns clearly complicate any effort to forecast the near-term probability of a major earthquake along the Plantain Garden fault, including whether some fault slip is accommodated by aseismic creep or whether other faults in eastern Jamaica accommodate some of the plate boundary slip. A worst-case forecast for a future rupture of the Plantain Garden fault assumes that the fault has not ruptured since 1692, that it is fully locked across a 15-km depth range, and that it accommodates all  $8\text{ mm yr}^{-1}$  of estimated fault slip in eastern Jamaica. In this case, the present seismic moment deficit would be equivalent to a  $M_w = 7.2$  earthquake if it were recovered in a single earthquake. This is comparable to the maximum magnitude rupture ( $M_w = 7.0\text{--}7.3$ ) observed for similar-length faults elsewhere, implying that the Plantain Garden fault may be near the end of its seismic cycle. This conclusion is not substantially altered if the  $M_w \sim 6.5$  1907 earthquake ruptured the Plantain Garden fault given that this earthquake relieved only 10 per cent of the elastic strain that had accumulated since 1692.

### 5.1.2 Central and western Jamaica

Recurrence intervals in central and western Jamaica are more difficult to estimate because of the likelihood that deformation is accommodated by multiple faults in these regions. The likely absence of significant earthquakes in central Jamaica since at least the late 17th century suggests a higher probability for significant rupture there than in western Jamaica, where the 1957 earthquake relieved some of the elastic strain that has accumulated during the past century. None of the morphologically prominent faults in central Jamaica that are described by previous authors, including the Rio Minhó-Crawle River fault zone of central Jamaica, the Duanvale fault of northern Jamaica, or South Coastal fault of southern Jamaica. (e.g. Wadge & Dixon 1984; Mann *et al.* 1985) have continuous traces longer than 70 km. Maximum moment magnitudes for faults in central Jamaica are thus likely to be comparable to that for the Plantain Garden fault of eastern Jamaica. If elastic strain has been accumulating in central Jamaica for at least the past 300 yr (since 1692) and we simplistically assume that the full  $8\text{ mm yr}^{-1}$  of fault slip in that region occurs along a single, 70 km-long fault with a 10–15-km-deep seismogenic layer, the implied seismic moment deficit is equivalent to a  $M_w = 7.1\text{--}7.2$  earthquake.

Although the discussion above focuses on the dominance of sinistral shear in Jamaica, the existence of high topography and numerous faults at high angles to the predominant direction of GPS motion on the island strongly suggests that thrust faulting also poses a significant earthquake hazard. The seismically active and high Blue Mountains of eastern Jamaica are of particular concern given their proximity to the capital city; however, possible shortening across the poorly understood, but morphologically prominent Santa Cruz

and Spur Tree faults of western Jamaica could also result in large thrust faulting earthquakes.

## 5.2 Comparison to opening rates across the Cayman spreading centre

Our  $6 \pm 1\text{ mm yr}^{-1}$  minimum and  $11 \pm 1\text{ mm yr}^{-1}$  maximum estimate for Gonâve–North America Plate motion (Section 4.2) provide the first geodetic bounds on instantaneous seafloor spreading rates across the Cayman spreading centre, assuming that the Gonâve microplate is rigid or approximately rigid between Jamaica and the Cayman spreading centre. Spreading rates averaged over the past 3–10 Myr from the hard-to-interpret seafloor spreading magnetic anomalies in the Cayman Trough provide a useful basis of comparison for our geodetic results, albeit over a much different timescale. Macdonald & Holcombe (1978) estimate a long-term opening rate of  $20\text{ mm yr}^{-1}$  from an inversion of Cayman spreading centre magnetic anomalies, whereas Rosencrantz *et al.* (1988) estimate a slower  $12\text{--}15\text{ mm yr}^{-1}$  range of long-term opening rates from seafloor depth and seafloor age profiles and a different interpretation of the magnetic anomaly sequence. Leroy *et al.* (2000) reinterpret the Cayman Trough magnetic anomaly sequence and estimate an average opening rate of  $17\text{ mm yr}^{-1}$  over the past 24 Myr, intermediate between the rates estimated by Macdonald & Holcombe (1978) and Rosencrantz *et al.* (1988).

Our  $11 \pm 1\text{ mm yr}^{-1}$  estimate of the maximum short-term opening rate from GPS data is thus slower than most estimates of Cayman spreading centre opening rates that are based on marine geophysical data. A slowdown in opening rates across the Cayman spreading centre over the past few Myr could account for this difference. Such a slowdown would imply that an increasing fraction of Caribbean–North America motion has been transferred from the Oriente fault at the northern edge of the Gonâve microplate to the Walton–Plantain Garden–Enriquillo fault zone along its southern boundary over the past few million years, consistent with a model in which the Gonâve microplate is progressively detaching from the Caribbean Plate and accreting to the North American Plate (Mann *et al.* 1995). That our minimum estimated rate for Gonâve–Caribbean Plate motion of  $8 \pm 1\text{ mm yr}^{-1}$  exceeds geological estimates of the long-term deformation rate in Jamaica of  $3\text{--}7\text{ mm yr}^{-1}$  (Section 2.1) is further consistent with a model in which accelerating Gonâve–Caribbean Plate motion accompanies a slowdown of Gonâve–North America Plate motion.

An alternative explanation of the apparent difference in the rate of Gonâve–North American Plate motion estimated from our GPS data in Jamaica and marine magnetic data along the Cayman spreading centre is the possibility that several millimeters per year of east-west shortening of the Gonâve microplate occurs somewhere between Jamaica and the Cayman spreading centre. Active shortening across N–S-trending reverse faults that are imaged by multichannel seismic lines in the Cayman Trough north of Jamaica (Leroy *et al.* 1996) (Fig. 2) is consistent with this hypothesis, as are locally and teleseismically recorded earthquakes that extend north to the southern coast of Cuba (Moreno *et al.* 2002).

If the long-term opening rate for the Cayman spreading centre has averaged only  $12\text{ mm yr}^{-1}$ , equal to the lower bound estimated by Rosencrantz *et al.* (1988), and if the present rate of Gonâve–North American Plate motion is equal to our GPS-derived upper limit of  $11 \pm 1.1\text{ mm yr}^{-1}$ , then the long-term and geodetic estimates agree within errors. This would imply that motion of the Gonâve microplate and hence slip rates across its plate boundaries

have remained relatively steady for the past several Myr, including steady long-term Gonâve–Caribbean Plate motion at the minimum estimated rate of  $8 \pm 1 \text{ mm yr}^{-1}$  (Section 4.1.3).

A scenario in which Gonâve microplate motion has remained steady for at least the past several Myr has several implications for deformation in and near Jamaica. For example, the  $\sim 40 \text{ km}$  of integrated slip estimated by Burke *et al.* (1980) from offsets of E–W-striking faults in Jamaica would have required no more than 5 Myr to accumulate at the minimum estimated rate of  $8 \pm 1 \text{ mm yr}^{-1}$ . Similarly, not more than 7.5 Myr would have been required to open the  $\sim 60 \text{ km}$ -wide Morant pull-apart basin at the eastern end of the Plantain Garden fault between eastern Jamaica and western Hispaniola (Natural Disaster Research *et al.* 1999). In contrast, faulting and folding associated with the present tectonic regime in Jamaica are estimated to have started at  $\sim 10 \text{ Ma}$  (Burke *et al.* 1980), earlier than implied by the steady-motion model. The discrepancy between the above estimates implies that deformation began more recently than  $\sim 10 \text{ Ma}$  or that the geologically based estimates of total long-term deformation underestimate the total deformation and hence imply ages for the onset of deformation that are too recent.

In summary, the available data are consistent with a model in which Gonâve microplate motion relative to the Caribbean Plate has increased from 3 to  $7 \text{ mm yr}^{-1}$  over the past few Myr to a minimum rate of  $8 \pm 1 \text{ mm yr}^{-1}$  at present. This interpretation implies a corresponding slowdown through time of slip along structures that accommodate Gonâve–North America Plate motion (e.g. the Oriente fault and Cayman spreading centre). Conversely, the same observations can be interpreted as evidence for steady long-term Gonâve Plate motion, provided that

(i) the long-term opening rate across the Cayman spreading centre has been only  $11\text{--}12 \text{ mm yr}^{-1}$ , equal to the slowest rate interpreted by any previous authors from seafloor spreading anomalies in the Cayman Trough.

(ii) the present rate of Gonâve–North America motion equals the maximum ( $11 \pm 1.1 \text{ mm yr}^{-1}$ ) permitted by our GPS data

(iii) long-term Gonâve–Caribbean motion has been faster than published geological estimates of  $3\text{--}7 \text{ mm yr}^{-1}$  either because deformation started more recently than estimated by previous authors or because significant deformation not accounted for in previous studies has occurred along onshore or offshore faults.

### 5.3 Restraining bend deformation

The present pattern of seismicity in Jamaica (Fig. 3b) dictates that at least some of the strike-slip motion that enters southeastern Jamaica along the Plantain Garden fault steps northward to one or more faults west of and possibly north of Jamaica. The NNW-striking faults that transfer this motion between the E–W-trending strike-slip faults function as restraining bends that accommodate crustal shortening and uplift. The GPS velocity gradient from the southwestern to the northeastern ends of the island (Fig. 10a) supports such an interpretation, although our GPS velocity uncertainties are presently too large to determine the details of where and how that crustal shortening occurs. The high topography (Fig. 3a) and concentrated microseismicity (Fig. 3b) associated with the Blue Mountains of eastern Jamaica suggest that significant crustal shortening occurs there. Whether significant additional shortening occurs across the morphologically prominent Santa Cruz and Spur Tree faults of western Jamaica, or possibly other faults on the island is a target of our ongoing work.

## 6 FUTURE WORK AND CONCLUSIONS

The GPS and seismic observations described above resolve several first-order questions about Gonâve microplate motion. The Jamaican GPS sites move significantly relative to both the neighboring North American and Caribbean plates, thereby demonstrating the existence of the Gonâve microplate at high confidence levels. Our comparison of Jamaican GPS site motions to the motions of sites in the Caribbean Plate interior yields a minimum rate of  $8 \pm 1 \text{ mm yr}^{-1}$  for Gonâve–Caribbean Plate motion. Half or more of Caribbean–North American Plate motion is thus accommodated by faults located at the southern boundary of the Gonâve microplate. The implied maximum rate of Gonâve–North American Plate motion across the Oriente fault and Cayman spreading centre is  $11 \pm 1 \text{ mm yr}^{-1}$ , significantly slower than all but one published estimate of the long-term seafloor spreading rate across the Cayman spreading centre at the western end of the Gonâve microplate. Our preferred interpretation of the available geodetic and geological evidence is that the Gonâve microplate is being progressively transferred to the North American Plate, thereby implying that fault slip rates in Jamaica have increased through time while rates along the Oriente fault and Cayman spreading centre have decreased. Within the broad uncertainties of all the observations, we cannot however rule out a model in which Gonâve microplate motion has remained steady for no longer than the past 5 Myr. Our estimate of Gonâve microplate motion is consistent with a broadly constrained estimate of fault slip rates in Hispaniola at the eastern end of the Gonâve microplate (Calais *et al.* 2002).

In Jamaica, GPS site directions in both the Caribbean Plate reference frame and North American Plate reference frame are parallel within their  $1\text{--}2\sigma$  uncertainties to the predicted direction for Caribbean–North America motion. The mean *P*- and *T*-axes for 48 earthquakes since 1941 exhibit shallow plunges and directions  $45^\circ$  from the predicted plate slip direction, consistent with deformation dominated by strike-slip faulting. We conclude that deformation on the island is dominated by left-lateral shear along largely E–W striking strike-slip faults. Resolving the GPS-derived minimum Gonâve–Caribbean Plate velocity in Jamaica onto the island's major strike-slip faults predicts minimum fault-parallel motion of  $7 \text{ mm yr}^{-1}$  and fault-normal motion of  $3 \text{ mm yr}^{-1}$ . To what degree this low obliquity transpressional motion is partitioned and if so, what structures accommodate the fault-normal motion is unknown. The GPS site velocities change systematically along cross-island transects that are oriented normal and parallel to the island's major faults. We interpret these deformation gradients as evidence for the existence of interseismic elastic strain that is caused by one or more locked faults on the island. That a significant velocity gradient exists along a island-wide transect that crosses NNW-trending faults at high angles to the predominant WSW direction of GPS site motion strongly suggests that crustal shortening also occurs. These observations are consistent with Mann *et al.*'s (1985) geologically based interpretation of the island's neotectonics in the context of a major fault restraining bend.

Our work leaves unanswered important questions about the details of neotectonic deformation on the island. Most notably, the GPS velocity uncertainties are still too large to determine which faults are actively accumulating strain, whether some faults creep, and the deformation mechanisms by which slip is transferred northward across the restraining bend from the Plantain Garden fault in southeastern Jamaica to the Walton fault offshore from northwestern Jamaica. Future occupations of the GPS network should reduce site velocity uncertainties to levels that merit more detailed elastic

half-space modelling of deformation on the island. We are also installing additional GPS sites in areas of the island poorly sampled by the present network toward a better definition of the 2-D velocity gradient on the island. Palaeoseismologic studies of the island's major faults are clearly needed to determine which faults are active and their long-term slip rates. Such information would provide valuable feedback for future efforts to model the interseismic strain being measured with GPS.

## ACKNOWLEDGMENTS

We thank Florin Ionica and Paul Williams of the Earthquake Unit for gathering GPS data and Neal Lord for installing GPS sites and equipment. We thank Glenville Draper and an anonymous reviewer for comments that significantly improved the manuscript. We thank Raymond Wright of the Petroleum Corporation of Jamaica for his generous contribution of a field vehicle, driver, and facilities, all of which were instrumental in starting this project. We thank the Jamaican government for supporting our efforts through the Earthquake Unit. Support was provided by NSF grant EAR-0003550. Institutions that have granted hospitality and access to their property for this project are the Boscobel Aerodrome, Brown's Town Community College, Cave Valley Police, Jamaica Defence Force, Jamaica Civil Aviation and Ports authorities, Jamalco Alumina Works, Knox High School, Negril Golf Club, Northern Caribbean University, Portland Cottage Gun Club, Petroleum Corporation Of Jamaica, Tarentum Coffee Processing Plant, and Western Regional Health Authority.

## REFERENCES

- Altamimi, Z., Sillard, P. & Boucher, C., 2002. ITRF2000: a new release of the International Terrestrial Reference Frame for earth science applications, *J. geophys. Res.*, **107**, 2214, doi:10.1029/2001JB000561.
- Arden, D.D., 1975. Geology of Jamaica and the Nicaragua rise, in *The Ocean Margins and Basins, The Gulf of Mexico and the Caribbean*, Vol. 3, pp. 617–661, eds Nairn, A.E.M. & Stehli, F.G., Plenum, New York.
- Burke, K., Grippi, J. & Sengor, A.M.C., 1980. Neogene structures in Jamaica and the tectonic style of the northern Caribbean plate boundary zone, *J. Geol.*, **88**, 375–386.
- Calais, E. & Mercier de Lepinay, B., 1995. Strike-slip tectonic processes in the northern Caribbean between Cuba and Hispaniola (Windward Passage), *Mar. Geophys. Res.*, **17**, 63–95.
- Calais, E., Mazabraud, Y., Mercier de Lepinay, B., Mann, P., Mattioli, G. & Jansma, P., 2002. Strain partitioning and fault slip rates in the northeastern Caribbean from GPS measurements, *Geophys. Res. Lett.*, **106**, 1–9.
- DeMets, C., 2001. A new estimate for present-day Cocos-Caribbean plate motion: Implications for slip along the Central American volcanic arc, *Geophys. Res. Lett.*, **28**, 4043–4046.
- DeMets, C., Gordon, R.G., Argus, D.F. & Stein, S., 1990. Current plate motions, *Geophys. J. Int.*, **101**, 425–478.
- DeMets, C., Mattioli, G., Jansma, P., Rogers, R., Tenorio, C. & Turner, H.L., 2006. Present motion and deformation of the Caribbean plate: Constraints from new GPS geodetic measurements from Honduras and Nicaragua, *Geol. Soc. Am.*, in press.
- Draper, G. & Robinson, E., 1991. Dextral slip on NNW trending faults in central Jamaica: evidence of Neogene domino tectonics? (abstract), *Geological Society of Jamaica*, p. 2.
- Ghose, W.A. & Testamarta, M.M., 1983. Paleomagnetic results from sedimentary rocks in Jamaica: initial results, *J. Geol. Soc. Jamaica*, **22**, 16–24.
- Hanks, T.C. & Kanamori, H., 1979. A moment magnitude scale, *J. geophys. Res.*, **84**, 2348–2350.
- Heflin, M. *et al.*, 1992. Global geodesy using GPS without fiducial sites, *Geophys. Res. Lett.*, **19**, 131–134.
- Horsfield, W., 1974. Major faults in Jamaica, *J. Geol. Soc. Jamaica*, **14**, 31–38.
- Leroy, S., Mercier de Lepinay, B., Mauffret, A. & Pubellier, M., 1996. Structural and tectonic evolution of the eastern Cayman Trough (Caribbean Sea) from seismic reflection data, *AAPG Bull.*, **80**, 222–247.
- Leroy, S., Mauffret, A., Patriat, P. & Mercier de Lepinay, B., 2000. An alternative interpretation of the Cayman trough evolution from a reidentification of magnetic anomalies, *Geophys. J. Int.*, **141**, 539–557.
- Macdonald, K.C. & Holcombe, T.L., 1978. Inversion of magnetic anomalies and sea-floor spreading in the Cayman Trough, *Earth planet. Sci. Lett.*, **40**, 407–414.
- Malitzky, A. & Shapira, A., 1995. PC-SDP: a PC-based seismic data processing system, The Geophysical Institute of Israel.
- Mann, P. & Burke, K., 1984. Neotectonics of the Caribbean, *Rev. Geophys. Space Phys.*, **22**, 309–362.
- Mann, P., Draper, G. & Burke, K., 1985. Neotectonics of a strike-slip restraining bend system, Jamaica, in *Strike-slip deformation, basin formation, and sedimentation, Special Publication, SEPM 37*, pp. 211–226, eds Biddle, K. & Christie-Blick, N., SEPM, Tulsa.
- Mann, P., Taylor, F.W., Edwards, R.L. & Ku, T., 1995. Actively evolving microplate formation by oblique collision and sideways motion along strike-slip faults: an example from the northeastern Caribbean plate margin, *Tectonophysics*, **246**, 1–69.
- Mao, A., Harrison, C.G.A. & Dixon, T.H., 1999. Noise in GPS coordinate time series, *J. geophys. Res.*, **104**, 2797–2816.
- Marquez-Azua, B. & DeMets, C., 2003. Crustal velocity field of Mexico from continuous GPS measurements, 1993 to June 2001: implications for the neotectonics of Mexico, *J. geophys. Res.*, **108**, 2450, doi:10.1029/2002JB002241.
- Molnar, P. & Sykes, L.R., 1969. Tectonics of the Caribbean and middle America regions from focal mechanisms and seismicity, *Geol. Soc. Am. Bull.*, **80**, 1639–1684.
- Moreno, B., Grandison, M. & Atakan, K., 2002. Crustal velocity model along the southern Cuban margin: implications for the tectonic regime at an active plate boundary, *Geophys. J. Int.*, **151**, 632–645.
- Natural Disaster Research, Inc., Earthquake Unit, Mines & Geology Division, 1999. Kingston Metropolitan Area Seismic Hazard Assessment Final Report, Caribbean Disaster Mitigation Project, Organization of American States, www.oas.org/cdmp/document/kma/seismic/kma1.htm, 82 pp.
- Robinson, E., 1994. Jamaica, in *Caribbean Geology: An Introduction*, pp. 111–123, eds Donovan, S.K., Jackson, T.A., University of West Indies Publisher's Association, Kingston.
- Rosencrantz, E. & Mann, P., 1991. SeaMARC II mapping of transform faults in the Cayman Trough, Caribbean Sea, *Geology*, **19**, 690–693.
- Rosencrantz, E. & Sclater, J.G., 1986. Depth and age in the Cayman Trough, *Earth planet. Sci. Lett.*, **79**, 133–144.
- Rosencrantz, E., Ross, M. & Sclater, J., 1988. Age and spreading history of the Cayman Trough as determined from depth, heat flow, and magnetic anomalies, *J. geophys. Res.*, **93**, 2141–2157.
- Ruellan, E., Mercier-de-Lepinay, B., Beslier, M.-O., Sosson, M., Monnier, C., Leroy, S., Rowe, D. & Cruz Calderon, G., 2003. Morphology and tectonics of the Mid-Cayman spreading centre (CAYVIC cruise) (abstract), *Geophys. Res. Abs.*, **5**, 12 580.
- Sandwell, D.T. & Smith, W.H.F., 1997. Marine gravity anomaly from Geosat and ERS 1 altimetry, *J. geophys. Res.*, **102**, 10 039–10 054.
- Stein, S. & Gordon, R.G., 1984. Statistical tests of additional plate boundaries from plate motion inversions, *Earth planet. Sci. Lett.*, **69**, 401–412.
- Sykes, L.R., McCann, W.R. & Kafka, A.L., 1982. Motion of Caribbean plate during last 7 million years and implications for earlier Cenozoic movements, *J. geophys. Res.*, **87**, 10 656–10 676.
- Tomblin, J.M. & Robson, G.R., 1977. A catalogue of felt earthquakes for Jamaica, with references to other islands in the Greater Antilles, 1564–1971, Ministry of Mining and Natural Resources (Jamaica), Mines & Geology Division Special Publication No. 2, 243 pp.

- Van Dusen, S.R. & Doser, D.I., 2000. Faulting processes of historic (1917–1962)  $M \geq 6.0$  earthquakes along the north-central Caribbean margin, *Pure appl. Geophys.*, **157**, 719–736.
- Wadge, G. & Dixon, T.H., 1984. A geological interpretation of SEASAT-SAR imagery of Jamaica, *J. Geology*, **92**, 561–581.
- Wells, D.L. & Coppersmith, K.J., 1994. New empirical relationships among magnitude, rupture length, rupture width, rupture area, and surface displacement, *Bull. seism. Soc. Am.*, **84**, 974–1002.
- Wiggins-Grandison, M.D., 2001. Preliminary results from the new Jamaica seismograph network, *Seism. Res. Lett.*, **72**, 525–537.
- Wiggins-Grandison, M.D., 2004. Simultaneous inversion for local earthquake hypocentres, station corrections, and 1-D velocity model of the Jamaican crust, *Earth planet. Sci. Lett.*, **224**, 229–240.
- Wiggins-Grandison, M.D. & Atakan, K., 2005. Seismotectonics of Jamaica, *Geophys. J. Int.*, **160**, 573–580.
- Zumberge, J.F., Heflin, M.B., Jefferson, D.C., Watkins, M.M. & Webb, F.H., 1997. Precise point positioning for the efficient and robust analysis of GPS data from large networks, *J. geophys. Res.*, **102**, 5005–5017.